MATH498 Senior Project Report

Pushed-Pulled Front Transitions in Tumor Growth

Hana Herbawi 100059412

Supervisor(s): Dr. Haralampos Hatzikirou (P),
Dr. Denys Dutykh

Contents

1 Problem Statement: Tumor Invasion

With the emergence of interdisciplinary fields, scientists could utilize the power of mathematical modeling and physical interpretation to understand biological phenomena. One such phenomenon is collective dynamics in multicellular systems, such as organs or tissues, which is considered as the emergent behavior from the interactions between individuals who make up a population, i.e. interactions between cells. Collective dynamics can be understood through different Agent-Based Models (ABMs) such as on-lattice and off-lattice models, which consider the behavior of individual cells [1].

Cancer invasion emerges from collective dynamics, and understanding such process is crucial for controlling and limiting its growth/invasion rate. Mathematically, invasion is described by the propagation of fronts, which are shape-preserving traveling waves propagating at constant speed v. Front propagation can be modeled by systems of Reaction-Diffusion equations. These equations describe a dynamical system wherein diffusion, and reaction (birth) processes occur. These equations exhibit 3 types of behavior: pushed, pulled, and mixed, and are distinguished by the leading edge of the front. The front speed v corresponds to the invasion speed or the rate at which the tumor spreads [1, 2]. Mathematically, a front connects an unstable state to a stable state, which in the case of invasion, would mean non-invaded and invaded regions, respectively [2]. Figure 1 illustrates front propagation and its ecological counterpart.

In this report, we focus on tumor invasion and aim to describe such process using a discrete mathematical model. This report is structured as follows: in section 2 we review existing literature on cancer tumor modeling, focusing on ABMs, in section 3 we present foundational mathematical concepts, in section 4 we discuss our mathematical model, the BIO-LGCA, in section 5 we derive the corresponding PDE using mean-field analysis, in section 6 we present our simulation results, and we conclude with an outlook.

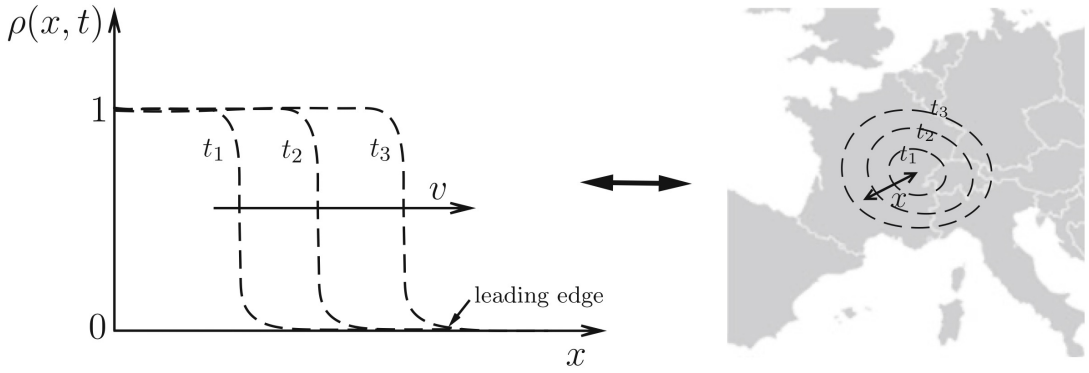

Figure 1. Front propagation and its ecological counterpart for the case of a biological invasion advancing in the radial direction r with a propagation speed v. Dashed lines represent the increasing spatial range of a species at different times [2].

2 Literature Review

Cancer is a disease that affects tissue in multi-cellular organisms and is characterized by uncontrollable cell division and the ability to invade adjacent and remote tissue [3]. Its heterogeneity increases its ability to test adaptation strategies under microenvironmental stresses, which, combined with its invasion capabilities, contributes to its fatality [4].

We have 2 main modeling approaches for understanding tissue dynamics: agent-based models (ABMs), where cells are regarded as individual units, and continuum methods, where cell individuality is discarded and tissue dynamics are derived from mesoscopic or macroscopic conservation and constitutive laws which draw parallels to physical systems [1, 5]. In this report, we will focus on agent-based models, which are ideal for capturing tissue dynamics as they mimic real life since cells are discrete entities. Distinct cell phenotypes may be taken into account as they may be crucial for analyzing the organization at the tissue level [1].

ABMs are classified into 2 main paradigms: on-lattice models, which restrict the movement of cells to an underlying lattice/grid, and off-lattice models, which have no such restriction [1, 4]. A third classification may be introduced which is the hybrid discrete-continuum model and is discussed in [5].

2.1 On-Lattice Models

On-lattice models are classified by the type of lattice/mesh used to discretize, or by their spatial resolution. A model can either have a regular or an irregular lattice. Regular lattices are easier to implement, visualize, and combine with partial differential equation solvers, but can lead to grid biases. Irregular lattices are more complex but ensure there are no grid biases [4].

On-lattice ABMs can be classified by their spatial resolution (operating on space-fixed lattices) into Cellular Automata (CA), Lattice-Gas Cellular Automata (LGCA), and Cellular Potts models (CPMs). CA models consist of a regular lattice where a single node (lattice site) can hold one cell. At each time-step, each cell is updated following specific rules which are proliferation, death, and migration. These rules depend on the states of neighboring nodes and a deterministic or stochastic transition function [1, 4, 5].

LGCA models allow a single node to hold multiple cells, where each node also contains velocity channels. LGCA models track the number of cells moving through the channels between individual nodes rather than the motion of each cell individually, which makes such models useful for efficiently simulating large numbers of cells over prolonged periods while also connecting to statistical mechanics theory, which provides a bridge between agent-based mathematical modeling and continuum methods involving systems of partial differential equations that model cell densities/populations rather than single cells [4]. Both CA and LGCA can mimic volume exclusion effects [1].

Some problems may require the resolution of individual cell morphologies [4]. CPM is a modeling method that uses an energy functional generalized from the Potts model to evaluate a multi-cellular state. The Potts model is a generalization of the Ising model, both of which are used to describe phenomena in solid state physics e.g., ferromagnets. In CPMs, several neighboring nodes represent a single cell and can qualitatively capture cell deformation, which has made CPMs a popular tool for modeling morphogenic processes such as cell sorting, cancer and tumor growth, and angiogenesis [5]. Although CPMs can model cell morphologies and mechanics, they are more computationally intensive [4].

All three on-lattice modeling approaches can describe the effects of mechanical forces of one cell on its neighbor, or on a group of neighboring cells to some extent which is why

they are used to describe collective dynamics [1].

2.2 Off-Lattice Models

In off-lattice models, cells are not restricted by an underlying lattice, rather, interactions between cells are described by forces or potentials. Cell position changes can be obtained by solving an equation of motion for each cell. Alternatively, the dynamics of a system of cells can be mimicked through energy-based methods using numerical procedures such as Monte Carlo sampling and the Metropolis algorithm [5]. Off-lattice models can be divided into center-based models (CBMs), and Deformable cell models, and vertex models.

CBMs focus on the volume (or masses) of cells [4]. In this model, cells are represented by simple geometrical objects that can be described by one or a small number of centers, with the basic assumption that each trajectory of a cell in space can be described by an equation of motion in formal analogy to physical particles [5].

The advantages of force-based models are a well-defined time scale and a more intuitive way of taking into account complex interactions of cells with other cells or their environment which is why they became the standard approach [5]. The second type of off-lattice models, Deformable cell models, and vertex models, is discussed in [5].

ABMs can track single-cell traits and individual behavior, which makes them well-suited for problems where single-cell effects are important such as heterogeneity and invasion. On-lattice models are easy and fast to implement, making them ideal for quick hypothesis testing, however, they may display some grid bias. Off-lattice models on the other hand, can readily incorporate biomechanics and off-lattice cell-cell interactions, however, they are more computationally intensive due to the need to calibrate many parameters [4]. Figure 2 classifies the ABMs we have mentioned in this section.

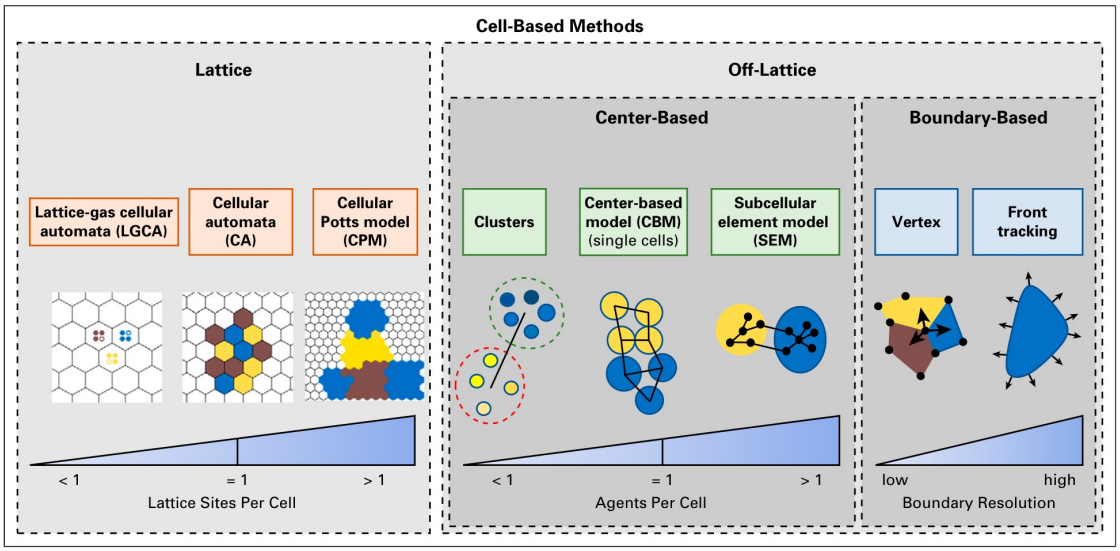

Figure 2. A schematic classification of cell-based modeling approaches [4].

3 Mathematical Foundations

This section provides the mathematical knowledge needed for our discussion. We will mainly present concepts from stochastic processes.

Definition 3.1 *A Stochastic Process is a set of random variables $X(t)$ defined on a common probability space $(\Omega, \mathcal{F}, \mathcal{P})$, with Ω being the sample space, $\mathcal{F}$ a σ-algebra, and $\mathcal{P}$ a probability measure indexed by a variable $t \in \mathbb{R}$ (usually time) where $X(t) \in \mathbb{Z}^n$ (discrete) or $X(t) \in \mathbb{R}^n$ (continuous).*

Definition 3.2 *A Markov Chain is a discrete stochastic process $X(t)$ that has memory only of its immediate past.*

Definition 3.3 *A Transition Probability is the probability that describes the evolution of the Markov Chain from $X(t_i) \in \mathbb{Z}^d$ to $X(t_j) \in \mathbb{Z}^d$ given $i, j \in \{1, \cdots, N\}$, where d the dimension of the random variable.*

$$
\begin{aligned}
&P(X(t) = j \mid X(t_1) = i, \cdots, X(t_n) = i_n) \\
=&P(X(t) = j \mid X(t_n) = i_n),\ \forall n > 1 \text{ and } 0 \leqslant t_1 \leqslant \cdots \leqslant t_n \leqslant t
\end{aligned} \tag{1}
$$

Definition 3.4 *A Transition Matrix is the matrix that collects all finite state transitions within a time-step.*

$$
\mathbf{P} = (P_{ij}) \in M^{N \times N}, P_{ij} = P(X(t + \tau) = j \mid X(t) = i) \tag{2}
$$

where $\sum_{j=1}^{N} P_{ij} = 1$ is the Stochastic Matrix.

Definition 3.5 *A Stochastic Matrix is a square matrix* $\boldsymbol{P}$ *with the following properties,*

1. $P_{ij} \geqslant 0, \forall\ i, j \in \{1, \cdots, N\}$
2. $\sum_j P_{ij} = 1$ for all i.

Definition 3.6 *The Continuous Master Equation is given by:*

$$
\dot{P}(x, t) = \int (\omega(x \mid z) P(z, t) - \omega(z \mid x) P(x, t))\, dz \tag{3}
$$

where $\dot{P}(x, t)$ *is the probability change,* $\omega(x \mid z)\ P(z, t)$ *is the influx, and* $\omega(z \mid x)\ P(x, t)$ *is the outflux.*

Definition 3.7 *The Discrete Master Equation is given by:*

$$
\dot{P}(n, t) = \sum_{n'} (\omega(n \mid n') P(n', t) - \omega(n' \mid n) P(n, t)) \tag{4}
$$

Example: *Poisson Process Master Equation*

$$
\dot{P}(n, t) = \lambda P(n - 1, t) - \lambda P(n, t)) \tag{5}
$$

The first moment (expectation/mean value) of the Master Equation:

$$\begin{aligned} < \dot{n} > &= \sum_{n=0}^{\infty} n\dot{P}(n,t) \\ &= \lambda \sum_{n} nP(n-1,t) - \lambda \sum_{n} nP(n,t) \end{aligned} \tag{6}$$

Using the following change of variable

$$\sum_{n} nP(n-1,t) \xrightarrow[n=n'+1]{n'=n-1} \sum_{n'}(n'+1)P(n',t) = \sum_{n} nP(n,t) + \sum_{n} 1P(n,t) \tag{7}$$

We get:

$$< \dot{n} >= \lambda < n > +\lambda - \lambda < n > \Longleftrightarrow < \dot{n} >= \lambda \Longleftrightarrow < n >= \lambda t + n_0 \tag{8}$$

Example: *One-Step Birth/Death Process*

Assume the following transition probabilities:

$$\omega^{+}(n) = \omega(n+1 \mid n) \tag{9}$$

$$\omega^{-}(n) = \omega(n-1 \mid n) \tag{10}$$

The corresponding master equation reads:

$$\dot{P}(n,t) = \omega^{+}(n-1)P(n-1,t) + \omega^{-}(n+1)P(n+1,t) - (\omega^{+}(n) + \omega^{-}(n))P(n,t). \tag{11}$$

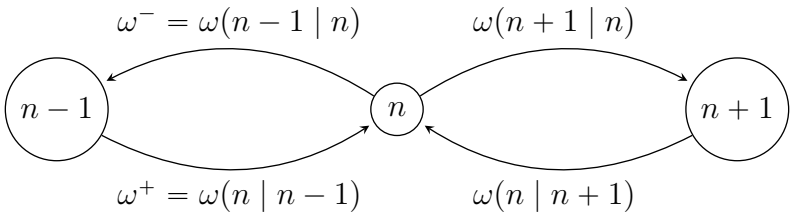

Figure 3. The Markov Chain Diagram

The first moment of the master equation reads as follows:

$$\begin{aligned}\sum_{n=\omega}^{\infty} n\dot{P}(n,t) = &\sum_{n=0}^{\infty} n(\omega^{+}(n-1)P(n-1,t) \\ &+ \sum_{n=0}^{\infty} n(\omega^{-}(n+1)P(n+1,t) \\ &- \sum_{n=0}^{\infty} n(\omega^{+}(n)+\omega^{-}(n))P(n,t) \end{aligned} \tag{12}$$

The first term on the RHS becomes:

$$\begin{aligned}\sum_{n=0}^{\infty} n(\omega^{+}(n-1)P(n-1,t) &\xrightarrow[n=n'+1]{n'=n-1} \sum_{n'=-1}^{\infty} (n'+1)(\omega^{+}(n')P(n',t) \\ &\xrightarrow[n=n']{n'=n} \sum_{n=0}^{\infty}(n)(\omega^{+}(n)P(n,t) + <\omega^{+}(n)> \end{aligned} \tag{13}$$

Similarly:

$$\begin{aligned}\sum_{n=0}^{\infty} n(\omega^{-}(n+1)P(n+1,t) &\xrightarrow[n=n'-1]{n'=n+1} \sum_{n'=1}^{\infty} (n'-1)(\omega^{-}(n')P(n',t) \\ &\xrightarrow[n=n']{n'=n} \sum_{n=0}^{\infty}(n)(\omega^{-}(n)P(n,t) - <\omega^{-}(n)> \end{aligned} \tag{14}$$

where we assumed that for $n'=0$, we get $n'\omega^{\pm}(n', P(n',t)) = 0$. Thus, we get:

$$<\dot{n}> = <\omega^{+}(n)> - <\omega^{-}(n)> . \tag{15}$$

Deriving the Diffusion Equation from the Master Equation:

Let the transition probabilities be:

$$\begin{aligned}\omega^{+(x-a)} &= \omega(x \mid x-a) = \frac{1}{2\tau} \\ \omega^{-(x+a)} &= \omega(x \mid x+a) = \frac{1}{2\tau}\end{aligned}$$

The corresponding Master Equation reads:

$$\begin{aligned}
&\dot{P}(x,t) = \omega^+(x-a)P(x-a,t) + \omega^-(x+a)P(x+a,t) - (\omega^+(x)+\omega^-(x))P(x,t) \\
\iff &\dot{P}(x,t) = \frac{1}{2\tau}P(x-a,t) + \frac{1}{2\tau}P(x+a,t) - P(x,t)
\end{aligned}$$

Expanding for small jumps $a \ll 1$:

$$\begin{aligned}
P(x-a,t) &= P(x,t) - a\frac{\partial P}{\partial x}(x,t) + \frac{a^2}{2}\frac{\partial^2 P}{\partial x^2}(x,t) \\
P(x+a,t) &= P(x,t) + a\frac{\partial P}{\partial x}(x,t) + \frac{a^2}{2}\frac{\partial^2 P}{\partial x^2}(x,t)
\end{aligned}$$

Then we get:

$$\begin{aligned}
\dot{P}(x,t) &= -P(x,t) + \frac{1}{2\tau}\left(P(x,t) - a\frac{\partial P}{\partial x}(x,t) + \frac{a^2}{2}\frac{\partial^2 P}{\partial x^2}(x,t)\right) \\
&\quad + \frac{1}{2\tau}\left(P(x,t) + a\frac{\partial P}{\partial x}(x,t) + \frac{a^2}{2}\frac{\partial^2 P}{\partial x^2}(x,t)\right) \\
&= \frac{a^2}{2\tau}\frac{\partial^2 P}{\partial x^2}(x,t) \qquad (16)
\end{aligned}$$

where eq. (16) becomes

$$\dot{P}(x,t) = D\frac{\partial^2 P}{\partial x^2}(x,t) \qquad (17)$$

which is the Diffusion Equation with diffusion constant $D = \frac{a^2}{2\tau} = \text{constant}$ for $a, \tau \to 0$. This is true only if $a = \epsilon$ and $\tau = \epsilon^2$, where $\epsilon \to 0$. This is called diffusive scaling.

Definition 3.8 *The Reaction-Diffusion Equation is given by:*

$$\frac{\partial \rho}{\partial t} = D\frac{\partial^2 \rho}{\partial x^2} + F(\rho) \qquad (18)$$

where $F(\rho)$ represents the reaction term. Setting $F(\rho) = 0$, we get diffusion, setting $F(\rho) = \tilde{r}\rho\left(1 - \frac{\rho}{K}\right)$ we get logistic reaction, and setting $F(\rho) = \tilde{r}\rho(1-\rho)\left(\rho + \alpha\right)$, we get Nagumo reaction [6].

4 The BIO-LGCA Model

The Biological Lattice-Gas Cellular Automata (BIO-LGCA) model is an on-lattice ABM for collective cell migration. It is characterized by synchronous time updates, and the explicit consideration of individual cell velocities [1]. BIO-LGCA is defined by a discrete spatial lattice $\mathcal{L}$, a discrete state space $\mathcal{E}$, a neighborhood $\mathcal{N}$, and local rule-based dynamics. Descriptions of $\mathcal{L}$, $\mathcal{E}$, and $\mathcal{N}$ can be found in [1].

4.1 LGCA Dynamics

In CA, certain local rules govern cell dynamics. Such rules determine the next state of each node based on its current state and on the state of its neighborhood. In order to determine a new lattice configuration, the local rule is applied independently and simultaneously at every node $\mathbf{r}$ of the lattice. Such rules are mathematically interpreted as transition probabilities $P(\mathbf{s} \to \mathbf{s}')$, where $\mathbf{s}$ is the pre-interaction node configuration and $\mathbf{s}'$ is the post-interaction node configuration [1].

These rules are composed of a combination of the following operators:

1. Stochastic Reorientation ($\mathcal{O}$)
2. Phenotypic Switching ($\mathcal{S}$)
3. Stochastic Cell Birth & Death ($\mathcal{R}$)
4. Deterministic Propagation ($\mathcal{P}$)

Together, ($\mathcal{P}$) and ($\mathcal{O}$) define cell movement, while ($\mathcal{S}$) allows cells to stochastically and reversibly transition between phenotypes.

In a BIO-LGCA, the stochastic operators are applied sequentially to every node, such that the transition probability can be expressed as

$$P(\mathbf{s} \to \mathbf{s}') = P_{\mathcal{S}} P_{\mathcal{R}} P_{\mathcal{O}}$$

where $P_i, i \in \{\mathcal{S}, \mathcal{R}, \mathcal{O}\}$ are the transition probabilities of the corresponding operator.

Therefore, we get $\mathbf{s}'$, the post-interaction node configuration, from the application of these stochastic operators, i.e. $\mathbf{s}' = \mathbf{s}^{\mathcal{S}\circ\mathcal{R}\circ\mathcal{O}}$.

Subsequently, the deterministic propagation operator ($\mathcal{P}$) is applied, and cells occupying velocity channels at the node, i.e. moving cells, are translocated to neighboring nodes in the direction of their respective velocity channels. The time-step increases once ($\mathcal{P}$) is applied [1].

The dynamics of the BIO-LGCA are illustrated in Figure 4, and are expressed by the following stochastic microdynamical equation:

$$\mathbf{s}_j(\mathbf{r} + \mathbf{c}_j, k+1) = \mathbf{s}'_j(\mathbf{r}, k)$$

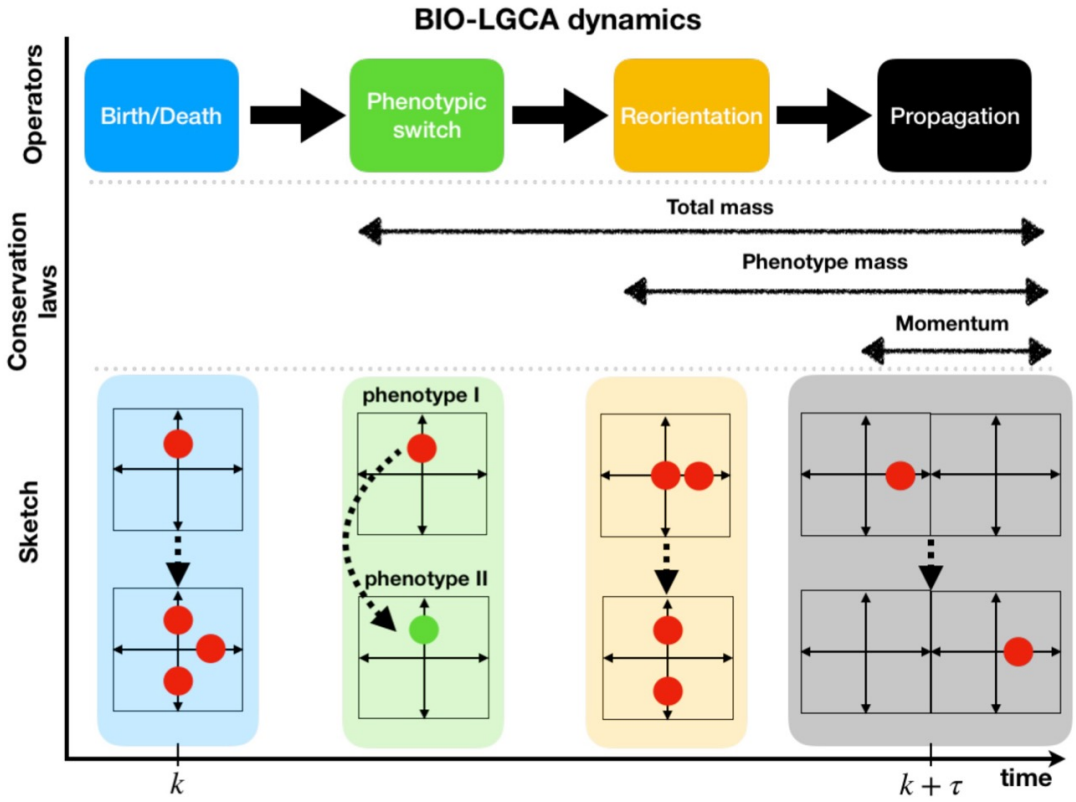

Figure 4. Operator-based dynamics of the BIO-LGCA. Propagation ($\mathcal{P}$), reorientation ($\mathcal{O}$), phenotypic switch ($\mathcal{S}$), and birth/death operators ($\mathcal{R}$) (top); conservation laws maintained by the different operators (middle); sketches of the operator dynamics (bottom) [1].

4.2 LGCA Model With Nagumo Reaction

Let $P_b(n \to n+1)$ denote the birth probability and $P_d(n \to n-1)$ denote the death probability.

P_b and P_d are defined as follows:

$$P_b = \tilde{r}\left(\frac{n}{K}\right)^2\left(1-\frac{n}{K}\right) + \tilde{r}\frac{\alpha}{K}\left(\frac{n}{K}\right)\left(1-\frac{n}{K}\right)\mathbb{I}(n+\alpha>0) \tag{19}$$

$$\tag{20}$$

$$P_d = \tilde{r}\frac{|\alpha|}{K}\left(\frac{n}{K}\right)\left(1-\frac{n}{K}\right)(1-\mathbb{I}(n+\alpha>0)) \tag{21}$$

where $K = b + \beta$ is the node capacity (the number of velocity channels (b) plus rest channels (β) per node), $\alpha \in \mathrm{R}$, and

$$\mathbb{I}(n+\alpha>0) = \begin{cases} 1, & n+\alpha>0 \\ 0, & n+\alpha \leqslant 0 \end{cases} \tag{22}$$

The condition $n + \alpha \leqslant 0$ can occur only for $\alpha < 0$. The mean-field reaction term $F(\rho)$, where the density $\rho = \frac{<n>}{K}$, is defined as follows:

$$F(\rho) =< P_b > - < Pd >= \begin{cases} \tilde{r}\rho(\rho+\alpha)(1-\rho), & \rho+\alpha>0 \\ \tilde{r}\rho(\rho-|\alpha|)(1-\rho), & \rho+\alpha \leqslant 0 \end{cases} \tag{23}$$

5 Mean-Field Analysis

5.1 Microdynamical Equations

In this section, we will demonstrate how to derive a spatio-temporal mean-field approximation of our LGCA reaction model for a spatially distributed system where we have finite diffusion strength ($< \infty$). This derivation was adapted from [7], which presents the

derivation for a general reaction term $F(\rho)$.

We begin with defining the occupation number for channel i, $\eta_i(\mathbf{r}, k)$ to be a binary variable

$$\eta_i(\mathbf{r}, k) \in \{0, 1\} \tag{24}$$

and the node density $n(\mathbf{r}, k)$ to be

$$n(\mathbf{r}, k) = \sum_{i=1}^{K} \eta_i(\mathbf{r}, k). \tag{25}$$

where the probability of having an occupied channel is given by:

$$f_i(\mathbf{r}, k) = P(\eta_i(\mathbf{r}, k) = 1) = \frac{n(\mathbf{r}, k)}{K} \tag{26}$$

In our model, we take into account cell birth and death. For the creation of a new cell on a node, at least one free channel is required, and for the death of a cell, we need at least one occupied channel. This condition can be formulated as follows:

$$\mathcal{R}_i(\mathbf{r}, k) = \xi_i(\mathbf{r}, k)(1 - \eta_i(\mathbf{r}, k)) - \xi_i(\mathbf{r}, k)(\eta_i(\mathbf{r}, k) \tag{27}$$

where $\xi_i(\mathbf{r}, k)$ are random Boolean variables corresponding to birth probabilities.

The corresponding microdynamical equations, which take an existing node configuration and apply certain operators in each time-step, read as follows:

$$\eta_i^{\mathcal{R}}(\mathbf{r}, k) = \eta_i(\mathbf{r}, k) + \mathcal{R}_i(\mathbf{r}, k) \tag{28}$$

$$\eta_i(\mathbf{r} + m\mathbf{c}_i, k + \tau) = \sum_{j=1}^{K} \mu_j(\mathbf{r}, k)\eta_j^R(\mathbf{r}, k). \tag{29}$$

where eq. 28 refers to the application of the *reaction* operator ($\mathcal{R}$) on the node occupation, where it assigns a new occupation number for a given channel through reaction, and eq. 29 refers to the node configuration after the application of the $\mathcal{R}$ operator in addition to the $\mathcal{O}$ operator, corresponding to the *redistribution* of cells on the velocity channels

and the $\mathcal{P}$ operator, corresponding to *propagation* to the neighboring nodes, where the application of both operators corresponds to diffusion.

5.2 Mean-Field Analysis of the Reaction LGCA

The main idea of mean-field analysis is that collective behavior can be approximated by taking the average behavior of the individuals. Note that this holds for large populations, which is the case when describing tumors, since they are made of a large number of cancer cells.

In order to get the corresponding PDE, we start by averaging over the system of microdynamical equations, 28 and 29, and then summing over the K channels:

$$\rho^{\mathrm{R}}(\mathbf{r}, k) = \rho(\mathbf{r}, k) + F(\rho(\mathbf{r}, k)) \tag{30}$$

$$\rho(\mathbf{r}, k + \tau) = \frac{1}{K} \sum_{j=1}^{K} \rho^{\mathrm{R}} \left(\mathbf{r} - m\mathbf{c}_j, k\right) \tag{31}$$

where $F(\rho) = \tilde{r}\rho\,(1-\rho)\,(\rho+\alpha)$ is the mean-field nagumo reaction term as defined in eq. 18. The first equation, eq. 30, accounts for the average change in the node density per time-step. The second eq. 31 describes how cells proliferate or die, in addition to being redistributed to the neighboring nodes, in 1 time-step.

Combining eq. 30 and 31, we get the following integrodifference equation, which describes how the node density $\rho(\mathbf{r}, k)$ is determined by integrating over all possible displacements within the lattice:

$$\rho(\mathbf{r}, k + \tau) = \int_{\mathcal{L}} \left[\rho\left(\mathbf{r} - m\mathbf{c}_i, k\right) + F\left(\rho\left(\mathbf{r} - m\mathbf{c}_i, k\right)\right)\right] \phi(m) dm \tag{32}$$

where $\phi(+m) = \phi(-m)$ is a symmetric redistribution kernel of the process, which physically means the cells can go in either direction with equal probability.

Integrating reaction term of eq. 32 yields:

$$\int_{\mathcal{L}} F\left(\rho\left(\mathbf{r}-m\mathbf{c}_i,k\right)\right)\phi(m)dm = \frac{\beta}{K}F(\rho(\mathbf{r})) + \frac{1}{K}\sum_{i=1}^{b} F\left(\rho\left(\mathbf{r}-m\mathbf{c}_i\right)\right) \tag{33}$$

$$= F(\rho(\mathbf{r})) + \frac{b}{K}\Delta_{\mathbf{r}} F\left(\rho\left(\mathbf{r}-m\mathbf{c}_i,k\right)\right) \tag{34}$$

where $\Delta_{\mathbf{r}} = \left[\sum_{i=1}^{b} F\left(\rho\left(\mathbf{r}-m\mathbf{c}_i\right)\right) - bF(\rho(\mathbf{r}))\right]/b$ is the discrete spatial Laplacian. The integral represents the average effect of the reaction term over all possible displacements m within the lattice, weighted by the redistribution kernel.

Expanding eq. 31 into a Taylor series and using eq. 34, we obtain the following PDE:

$$\frac{\partial\rho}{\partial t} = \frac{m^2}{K\tau}\nabla^2\rho + \frac{1}{\tau}F(\rho) + \frac{bm^2}{K\tau}\nabla^2 F(\rho). \tag{35}$$

Since we are interested in the long-term dynamics of the system, we use parabolic scaling where we assume that the $(\mathbf{x}, t)$ variables converge to 0, and we get the following PDE:

$$\frac{\partial\rho}{\partial t} = D\frac{\partial^2\rho}{\partial x^2} + \frac{1}{\tau}F(\rho) \tag{36}$$

where $D = m^2/K\tau$ is the diffusion rate, and $\tilde{r}$ the proliferation/growth rate.

6 Results

6.1 Simulating Tumor Dynamics

We start simulating the behavior of tumors by considering a thin strip of cells as our initial condition on a 140 by 20 lattice, mimicking growth in a tube. Running the simulation for 200 time-steps and plotting the density profile (Figure 5), we notice that the tumor has a low-density rim of proliferative cancer cells, where the cells invade neighboring tissue.

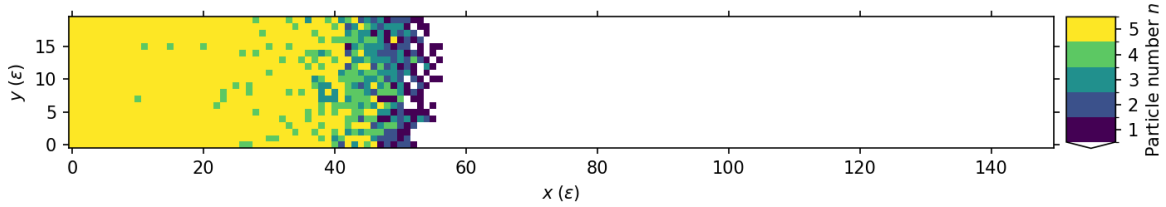

Figure 5. Simulation of Tumor Growth in a Tube.

6.2 Projecting the Simulation onto the X-Axis

In order to study the travelling front, we reduce our 2D system to 1D by averaging over the y-axis. We set the initial conditions to be a strip of cells just like the previous simulation, however, we elongate the lattice for a clearer display of the wave, and simulate it for 1000 time-steps, n times (where $n = 10$ in this case), and take the average to decrease the noise.

By plotting the 1-dimensional system (Figure 6), we get the average density based on front position, where density equal to 5 (our carrying capacity) corresponds to the "bulk" of the tumor, and then the density drops at the edge of the tumor, which corresponds to the low-density rim of proliferative cells that invade neighboring healthy tissue at a constant speed, as we will discuss shortly.

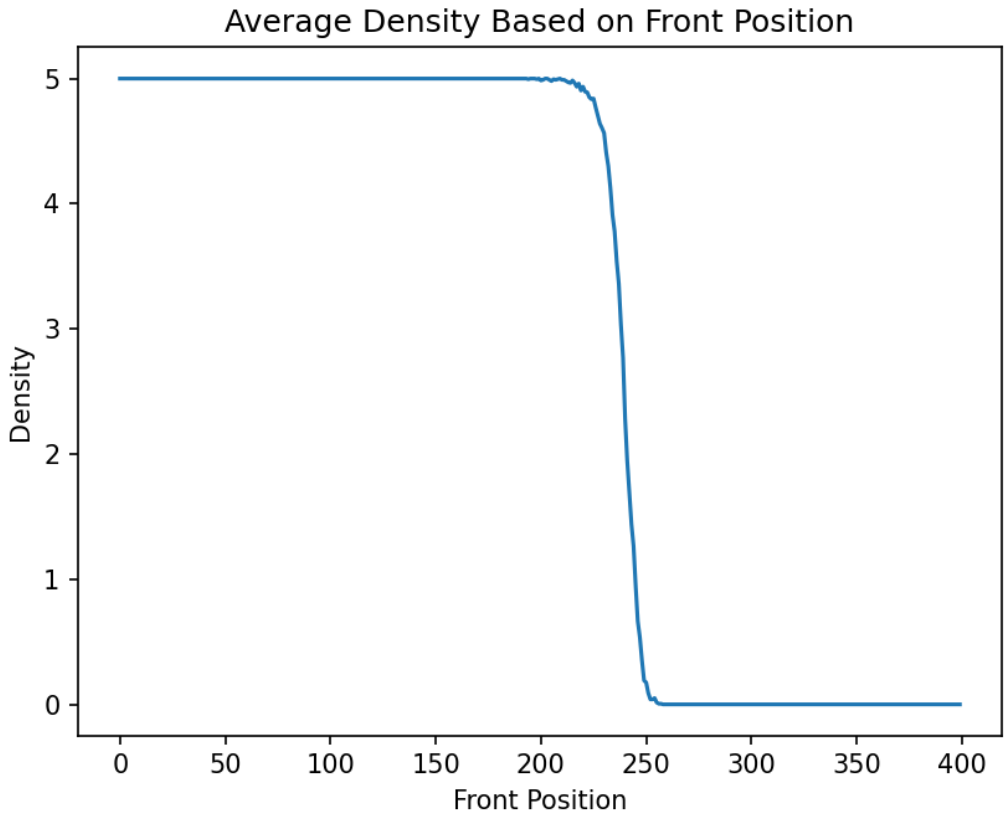

Figure 6. The average density of the tumor is based on its position, where high density corresponds to the bulk part of the tumor while low density corresponds to the low-density rim of the tumor [7].

6.3 Calculating the Front Speed

To calculate the front speed, we start by calculating the average density profile, and define the wavefront as the point where there is one cell on average. We then plot the evolution of the front position with time. Figure 7 shows that the front position evolves linearly with time, indicating that the tumor grows (invades healthy tissue) at a constant speed $v = 0.24$ (the slope of the linear fit). Note that the value of speed varies depending on the values of the parameters set in the simulation.

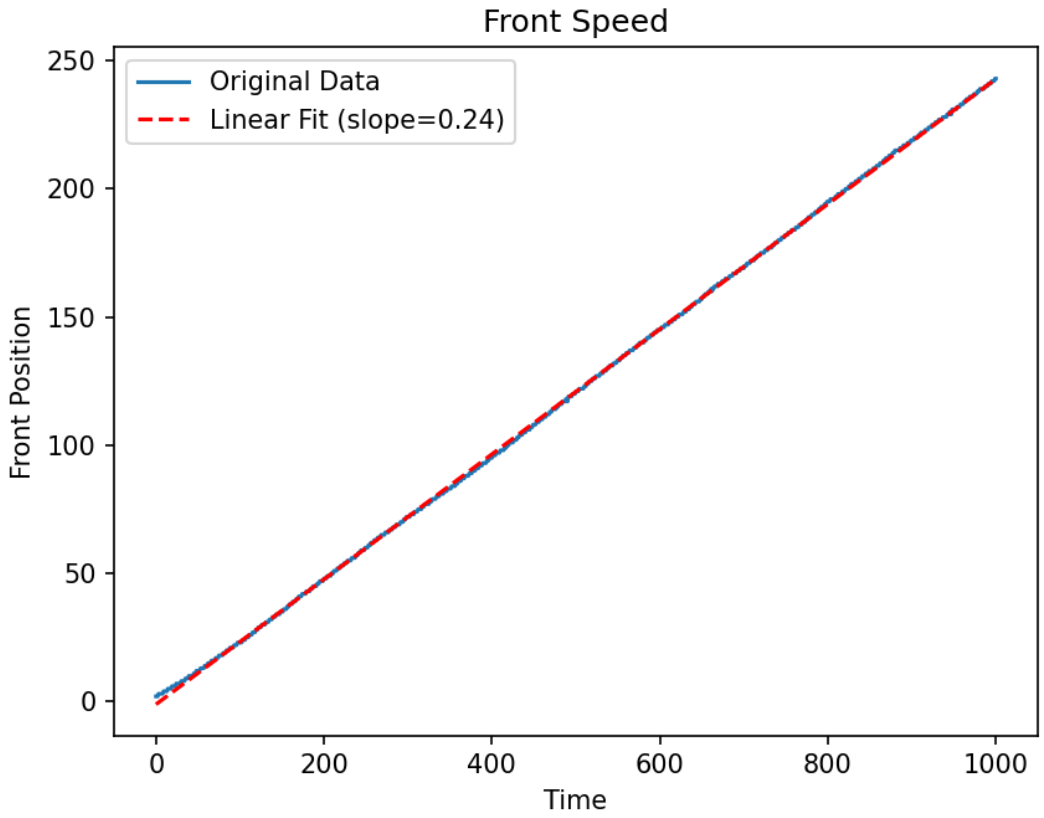

Figure 7. Front position evolves linearly with time indicating constant invasion speed.

7 Conclusion & Outlook

In this report, our aim was to further understand tumor dynamics, by modeling tumor behavior using the BIO-LGCA model. We discussed our problem statement, tumor invasion, and then presented the different types of mathematical models found in literature, in addition to mathematical prerequisites. We then explained our mathematical model, the BIO-LGCA model, and then proceeded to derive the corresponding PDE with Nagumo reaction using mean-field analysis. Finally, we presented our results from running simulations, where we simulated the growth of a tumor in a tube and plotted the tumor density profile, which coincided with tumors' behavior in real life, where they form a low-density proliferative rim for invasion, in addition to plotting the time evolution of the tumor position, to calculate the front speed, which was found to be constant.

In the future, we aim to compare our discrete model with the PDE approximation 36 by plotting the front speed for a narrow window of proliferation rates, where both models are expected to coincide for very small values of $\tilde{r}$. We also aim to compare the tumor speed at the bulk of the tumor, with the speed at the edge of the tumor. Finally, we would like to further discuss the biological interpretation of our findings in the context of pushed and pulled fronts in tumor invasion.

Code Availability

The code used to run the simulations can be found as an ipynb and an HTML file in this GitHub repository, along with this report.

References

1. Deutsch, A., Nava-Sedeño, J. M., Syga, S. & Hatzikirou, H. BIO-LGCA: a cellular automaton modelling class for analysing collective cell migration. *PLoS computational biology* **17,** e1009066 (2021).
2. Méndez, V., Campos, D. & Bartumeus, F. *Stochastic foundations in movement ecology* (Springer, 2016).
3. Kuznetsov, M., Clairambault, J. & Volpert, V. Improving cancer treatments via dynamical biophysical models. *Physics of life reviews* **39,** 1–48 (2021).
4. Metzcar, J., Wang, Y., Heiland, R. & Macklin, P. A review of cell-based computational modeling in cancer biology. *JCO clinical cancer informatics* **2,** 1–13 (2019).
5. Van Liedekerke, P., Palm, M., Jagiella, N. & Drasdo, D. Simulating tissue mechanics with agent-based models: concepts, perspectives and some novel results. *Computational particle mechanics* **2,** 401–444 (2015).
6. Mendez, V., Fedotov, S. & Horsthemke, W. *Reaction-transport systems: mesoscopic foundations, fronts, and spatial instabilities* (Springer Science & Business Media, 2010).
7. Hatzikirou, H. *Lattice-gas cellular automata models for the analysis of cancer invasion* PhD thesis (Dresden, Techn. Univ., Diss., 2009, 2009).